

Article

Extensional Flow Properties of Externally Plasticized Cellulose Acetate: Influence of Plasticizer Content

Stefan Zepnik ^{1,2,*}, Stephan Kabasci ¹, Rodion Kopitzky ¹, Hans-Joachim Radusch ² and Thomas Wodke ¹

¹ Department Bio-based Plastics, Fraunhofer Institute for Environmental, Safety, and Energy Technology UMSICHT, Osterfelder Straße 3, 46047 Oberhausen, Germany; E-Mails: stephan.kabasci@umsicht.fraunhofer.de (S.K.); rodion.kopitzky@umsicht.fraunhofer.de (R.K.); thomas.wodke@umsicht.fraunhofer.de (T.W.)

² Center of Engineering Sciences, Polymer Technology, Martin Luther University Halle-Wittenberg, 06099 Halle, Germany; E-Mail: hans-joachim.radusch@iw.uni-halle.de

* Author to whom correspondence should be addressed; E-Mail: stefan.zepnik@umsicht.fraunhofer.de; Tel.: +49-208-8598-1372; Fax: +49-208-8598-1290.

Received: 7 June 2013 / Accepted: 24 June 2013 / Published: 2 July 2013

Abstract: Elongational flow properties of polymer melts are very important for numerous polymer processing technologies such as blown film extrusion or foam extrusion. Rheotens tests were conducted to investigate the influence of plasticizer content on elongational flow properties of cellulose acetate (CA). Triethyl citrate (TEC) was used as plasticizer. Melt strength decreases whereas melt extensibility increases with increasing plasticizer content. Melt strength was further studied as a function of zero shear viscosity. The typical draw resonance of the Rheotens curve shifts to higher drawdown velocity and the amplitude of the draw resonance decreases with increasing TEC content. With respect to foam extrusion, not only are melt strength and melt extensibility important but the elongational behavior at low strain rates and the area under the Rheotens curve are also significant. Therefore, elongational viscosity as well as specific energy input were calculated and investigated with respect to plasticizer content. Preliminary foam extrusion tests of externally plasticized CA using chemical blowing agents confirm the results from rheological characterization.

Keywords: biopolymers; cellulose acetate; plasticizer; foaming; rheotens test; melt strength

1. Introduction

It is well known that for excellent foam extrusion performance the polymer must fulfill specific thermal and rheological properties. Adequate melt viscosity is necessary to maintain sufficient melt pressure in the die and to prevent premature foaming [1]. In this context, it has to be considered that the dissolved blowing agent (BA) can act as plasticizer, which causes a considerable reduction in the viscosity of the polymer melt [2–5]. If melt pressure is lower than the solubility pressure required for complete dissolution of the BA in the melt, early nucleation and premature foaming in the die can occur, causing poor morphology and surface quality of the foam [1,6,7]. Therefore, information on shear rheology of the polymer melt with and without dissolved blowing agent are essential. Due to strong biaxial stretching of the matrix material in the cell walls during bubbles expansion, sufficient extensional flow properties such as high melt strength and high melt extensibility are needed [1,2,8]. On one hand, if melt strength is too low cell wall rupture and cell coalescence can occur leading to low expansion ratios and inhomogeneous foam morphologies with high content of open cells [1,9,10]. On the other hand, extensively high melt strengths can hinder cell nucleation and cell growth, resulting in heterogeneous foam morphologies, too, and leading to high densities of the foamed product [9,10].

Polystyrene (PS) generally meets the above-mentioned requirements, and thus became the predominant polymer for foam extrusion applications such as insulation boards or foam sheets for packaging. However, PS is derived from petrochemicals and is non-renewable. Styrene as the basic building block of PS is regarded as potential hazardous chemical for example by the International Agency for Research on Cancer (IARC) [11–14]. As a consequence, PS does not fulfill all of the requirements for sustainability, which is becoming more and more important today.

Cellulose acetate (CA) as an organic cellulose ester is one of the oldest bio-based polymers. CA is non-toxic and is produced from cellulosic raw materials such as wood, cotton, sugarcane bagasse or recycled paper by a two-step esterification [15]. However, melt processing of CA requires certain modification of the material due to the narrow temperature window between its glass transition temperature T_g and its thermal degradation temperature T_d [16]. State of the art technology is external plasticization using low molecular weight plasticizers. Typical characteristics of externally plasticized CA such as amorphicity or mechanical properties are comparable to those of PS. This makes CA as a good candidate to replace PS in certain applications.

Comprehensive data are available concerning the influence of plasticizers on the properties of polymers such as cellulose esters, starch or poly(vinyl chloride) (PVC) [16–23]. Generally, the addition of low molecular weight plasticizers causes an increase in free volume, in lubricity, and in chain mobility of the polymer [23,24]. This is basically accompanied with a decrease in glass transition temperature T_g [23,24]. As a result, melt viscosity and viscoelasticity decrease whereas melt flow increases. Lots of research groups have studied the effect of plasticizers on melt processing and melt flow behavior of various polymers [25–27]. However, the plasticizer not only influences shear viscosity of the polymer melt, but also the extensional melt properties such as melt strength and melt elongation. Lin and Ku [28] studied extensional flow properties of externally plasticized poly(vinyl alcohol) (PVA). Elastic melt properties of externally plasticized PS were investigated in terms of extrudate swell by Qian *et al.* [25]. If extensional flow properties are poor due to too strong plasticization, reduced foam extrusion behavior of the polymer can be the consequence. Therefore,

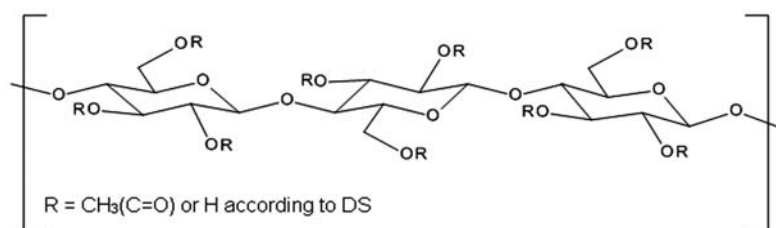
when discussing the suitability of CA for foam extrusion it is necessary to investigate the influence of plasticizer on thermal and rheological properties, especially on extensional flow behavior. To our knowledge, no systematic research has been published so far concerning the extensional flow properties of externally plasticized CA melts. This paper presents recent results of shear rheology and extensional flow properties of CA in dependence of plasticizer content. Preliminary foam extrusion tests using chemical blowing agents are also shown to verify the results from rheological characterization.

2. Experimental Section

2.1. Materials and Compounding

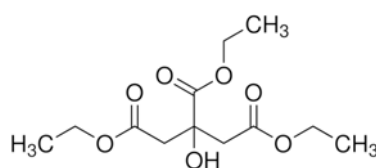
CA was obtained as white powder from Acetati SpA (Italy). Figure 1 shows the general structure of cellulose acetate. The degree of substitution (DS) is 2.5 and the density is $1.35 \text{ g}\cdot\text{cm}^{-3}$. The Hansen solubility parameter δ of CA (Cellidora A) is $24.5 \text{ MPa}^{0.5}$ [29].

Figure 1. General structure of cellulose acetate (CA).



Triethyl citrate (TEC) was obtained from Jungbunzlauer (Germany) as non-toxic and fully bio-based plasticizer. It has been reported by Mohanty *et al.* [16], that TEC is a good plasticizer for organic cellulose esters. The general structure of TEC is shown in Figure 2.

Figure 2. General structure of triethyl citrate (TEC).



Typical properties of TEC are listed in Table 1. Three concentrations, namely 15, 20, and 25 wt %, were used to investigate the influence on melt properties and principal foaming behavior of CA.

Table 1. Typical properties of triethyl citrate (TEC).

M_n ($\text{g}\cdot\text{mol}^{-1}$)	ρ ($\text{g}\cdot\text{cm}^{-3}$)	V_m ($\text{cm}^3\cdot\text{mol}^{-1}$)	T_{bp} at 706 mmHg ($^{\circ}\text{C}$)	Hansen solubility parameter δ [(MPa) ^{0.5}] [29]			
				δ_t	δ_d	δ_p	δ_h
276.3	1.13	244.5	294	20.98	16.5	4.9	12.0

Compounding was done using an intermeshing co-rotating twin-screw extruder EMP 26–40 from TSA Industriale (Italy). The screw diameter D is 26 mm and the screw length L is 40 D . The

throughput was kept constant at $10 \text{ kg}\cdot\text{h}^{-1}$ and the screw speed was set at 320 min^{-1} . The injection of the liquid plasticizer was done by means of a peristaltic pump between zone 2 and 3 of the extruder. Pressure and torque were measured during compounding and the specific mechanical energy input *SME* was calculated according to Equation (1) [30]:

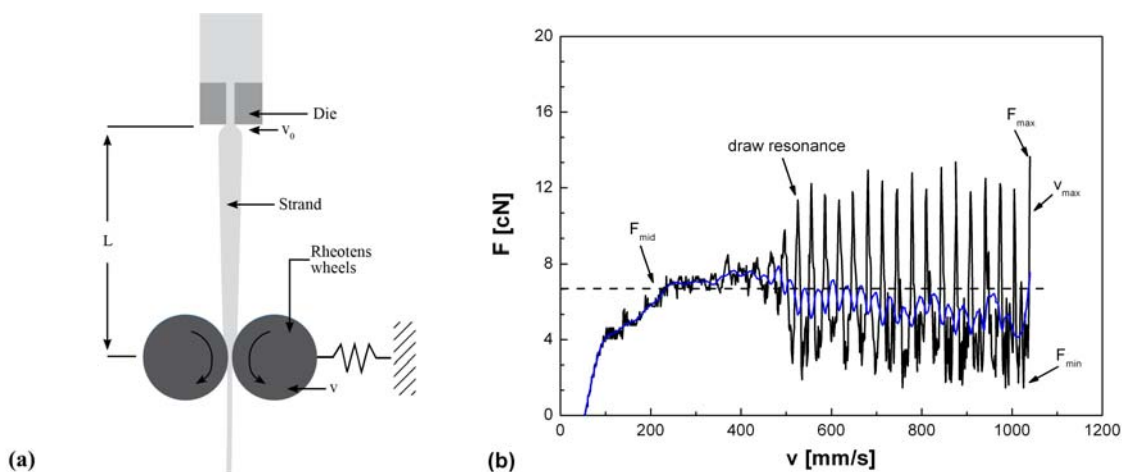
$$SME = \frac{\tau \cdot N}{\dot{m}} \text{ (kJ}\cdot\text{kg}^{-1}) \quad (1)$$

where τ is the torque (Nm), N is the screw speed (s^{-1}) and \dot{m} is the throughput ($\text{kg}\cdot\text{h}^{-1}$). Melt strands were extruded through a dual strand die ($d_0 = 3 \text{ mm}$) into a water bath. The strands were pelletized and dried for 6 h at $70 \text{ }^\circ\text{C}$.

2.2. Measurements

Shear rheology of externally plasticized CA was investigated by measuring the melt flow rate *MFR* and the shear viscosity η . The *MFR* was obtained at $220 \text{ }^\circ\text{C}$ and 5 kg load. Shear viscosity η at low shear rate was measured using a rotational rheometer (Bohlin Gemini, now Malvern) in cone-plate modus at $220 \text{ }^\circ\text{C}$ with a shear rate ranging from 0.01 to 100 s^{-1} . Film specimens with 0.2 mm thickness were prepared from the extruded compounds via compression molding at $197 \text{ }^\circ\text{C}$. Shear viscosity η at high shear rates was measured using a high pressure capillary viscometer (Göttfert) with a capillary die ($L/d_0 = 30/1$) and a shear rate ranging from 10 to 5000 s^{-1} . Uniaxial elongational flow properties were characterized by means of an extrusion system with a Rheotens device (Göttfert). A single screw extruder was used with a capillary die ($d_0 = 2 \text{ mm}$ and $L/d_0 = 30/2$) and a barrel temperature of $220 \text{ }^\circ\text{C}$. The throughput was kept constant at $0.5 \text{ kg}\cdot\text{h}^{-1}$. The extruded melt strand was grabbed and drawn down by a pair of rotating wheels, which is fixed to the Rheotens analyzer. A schematic sketch of the Rheotens test is shown in Figure 3a. The distance L between the die and the wheels of the Rheotens analyzer was set to 100 mm for all measurements. The drawdown velocity v was steadily increased with a constant acceleration rate of $24 \text{ mm}\cdot\text{s}^{-2}$. For reproducibility, five measurements were conducted at each plasticizer concentration and the average values were used for characterization. Figure 3b shows a typical Rheotens curve of externally plasticized CA as a function of drawdown velocity v .

Figure 3. (a) Schematic setup of the Rheotens test; (b) Typical Rheotens curve of externally plasticized CA: Drawdown force F as a function of drawdown velocity v .



The drawdown force $F(v)$ and the drawdown velocity v were investigated as a function of plasticizer content. Information on melt strength at low strain rate is important for polymer foaming. Therefore, extensional viscosities were calculated from the Rheotens curves according to an analytical model developed by Wagner *et al.* [31]. To gain further information on the extensional deformation at low strain rate, the initial slope of the stress curve $\sigma(V)$ at low draw ratio V was studied in dependence of plasticizer content. Muke *et al.* [32], Kao *et al.* [33], and Spoerrler *et al.* [34] investigated also this initial slope of the Rheotens curve for different test conditions. Herein, the draw ratio V is defined as the ratio of the strand velocity v between the Rheotens wheels and the die exit velocity v_0 that was calculated according to Equation (2) [35]:

$$v_0 = \frac{\dot{m}}{\rho \cdot A_0} \quad (\text{mm} \cdot \text{s}^{-1}) \quad (2)$$

where \dot{m} is the mass flow rate ($\text{g} \cdot \text{s}^{-1}$), ρ is the melt density ($\text{g} \cdot \text{mm}^{-3}$), and A_0 is the cross section of the die (mm^2). The initial slope of the stress curves was obtained by linear fit of the stress values corresponding to a stepwise increase in draw ratio V until the R^2 values became lower than 98%. Additionally, the influence of plasticizer content on typical draw resonance was studied. Extensional flow properties were further correlated to shear viscosity using the zero shear viscosity η_0 , which was obtained from rotational rheometry. Finally, the area under the Rheotens curve was used to calculate the specific energy input ΔG per unit mass and to define a foamability number FN according to Stadlbauer *et al.* [36].

2.3. Foam Extrusion Tests

Preliminary foam extrusion tests using chemical blowing agents (CBA) were conducted to verify the foamability of CA and to investigate the influence of plasticizer. Unicell TS was kindly supplied from Tramaco (Germany) as CBA. Typical properties of Unicell TS are listed in Table 2.

Table 2. Typical properties of Unicell TS.

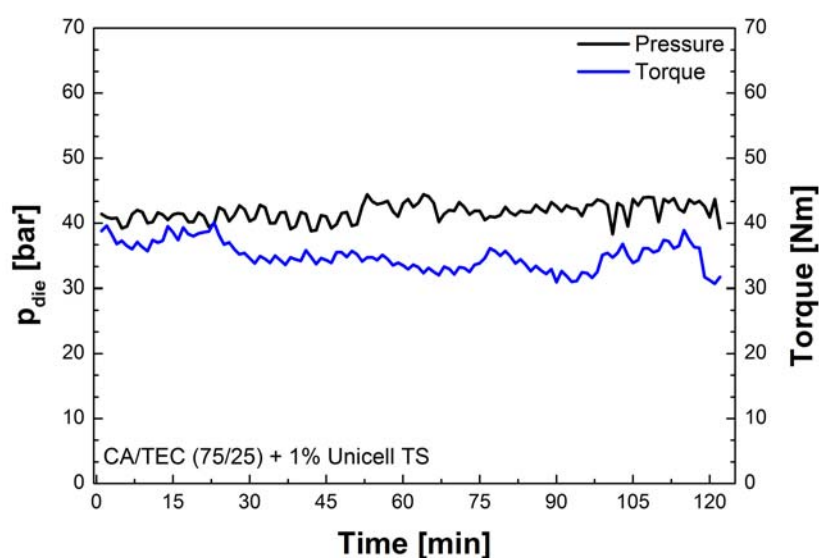
Property	Unicell TS
Name	para-toluene-sulfonyl-semicarbazide
Type of decomposition	exothermic
Decomposition temperature ($^{\circ}\text{C}$)	220
Gas yield at 220 $^{\circ}\text{C}$ ($\text{mL} \cdot \text{g}^{-1}$)	130
Foaming gas components	CO_2 , N_2 , NH_3
Average particle size (μm)	10

A single screw extruder ($D = 19$ mm and $L = 25 D$) with a strand die ($d_0 = 2$ mm) was used. To investigate the influence of plasticizer content on foam extrusion behavior of CA, the foam extrusion conditions and the CBA content were kept constant for 15, 20, and 25 wt % TEC. Table 3 shows the processing parameters used for chemical foaming of CA.

Table 3. Processing parameters for the foam extrusion tests of externally plasticized CA.

Unicell TS (wt %)	Screw speed (min ⁻¹)	Die pressure (bar)	Extruder barrel temperatures (°C)				
			1	2	3	4	Die
1	12	40	200	220	210	195	185

Five samples were collected for each compound under constant foam extrusion conditions. Figure 4 shows exemplarily torque and die pressure p_{die} of CA with 25 wt % TEC foamed with 1% Unicell TS. The foam morphology of the samples was investigated by means of scanning electron microscopy (SEM). Expansion behavior of the strands was characterized by the ratio of the strand diameter of the foam d_f to strand diameter of the non-foamed polymer d_p .

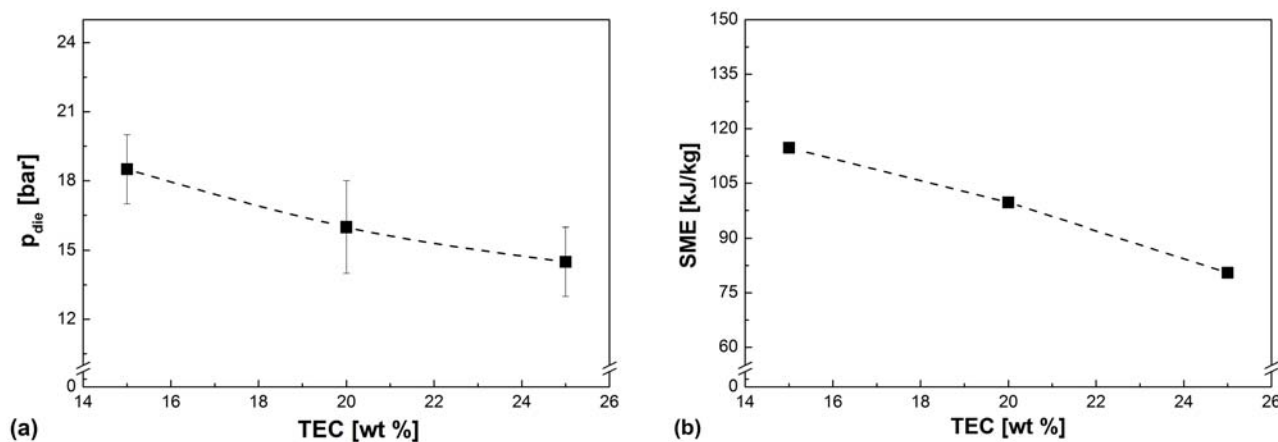
Figure 4. Torque and die pressure p_{die} as a function of extrusion time for CA/TEC (75/25) and 1% Unicell TS.

3. Results and Discussion

3.1. Influence of Plasticizer Content on Melt Processing of CA

Figure 5 shows the die pressure p_{die} and the specific mechanical energy input SME of externally plasticized CA during compounding. Die pressure p_{die} as well as SME show the same trend; both decrease with increasing plasticizer content. However, the influence of plasticizer content on SME is more pronounced. Similar dependencies for SME can be found in the literature for other plasticized polymers such as thermoplastic starch [37–39]. The addition of low molecular weight plasticizer results in the decrease of the intermolecular forces between the polymer chains due to shielding of functional (polar) groups along the polymer chains. That leads to an increase in free volume and chain mobility. As a result, the glass transition temperature T_g of CA decreases whereas melt flow rate increases. Improved melt processing can be achieved even at lower processing temperatures with less shear and less energy consumption [19].

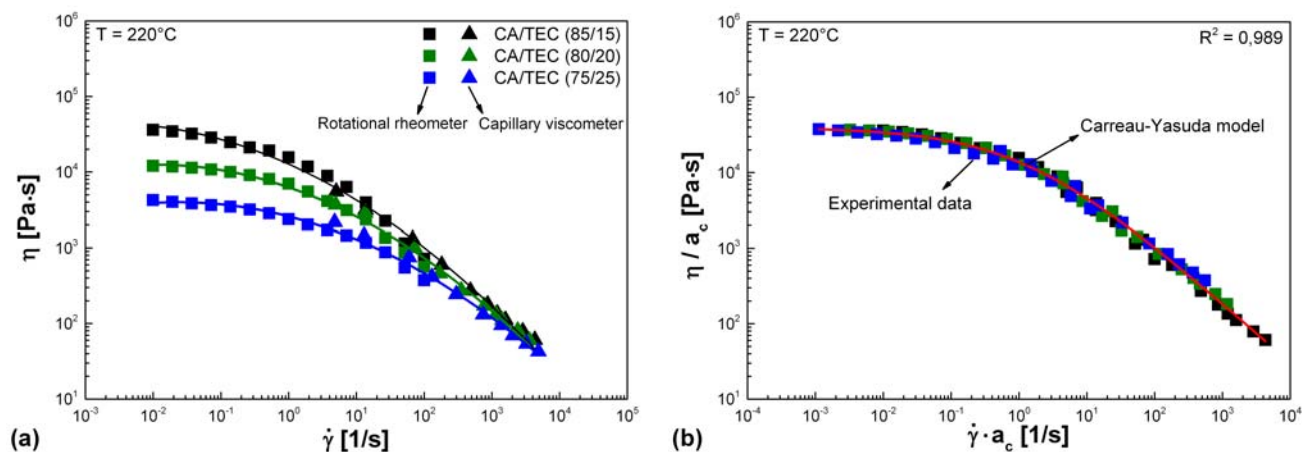
Figure 5. (a) Die pressure p_{die} as a function of TEC content; (b) Specific mechanical energy input SME as a function of TEC content.



3.2. Influence of Plasticizer Content on Shear Viscosity and Elongational Flow Properties of CA

Figure 6 shows the shear viscosity at 220 °C for externally plasticized CA in dependence of TEC content. As can be seen, shear viscosity decreases continuously with increasing plasticizer concentration due to stronger plasticization of CA. This is in good agreement with the previous results obtained for the die pressure and the specific mechanical energy input. The influence of plasticizer is more pronounced in the lower shear rate range whereas at higher shear rate its influence diminishes due to the shear thinning effect of the polymer melt.

Figure 6. (a) Shear viscosity η of externally plasticized CA as a function of shear rate $\dot{\gamma}$ in dependence of TEC content; (b) Calculated master curve using a concentration-dependent shift factor a_c and predicted master curve using the Carreau-Yasuda model.



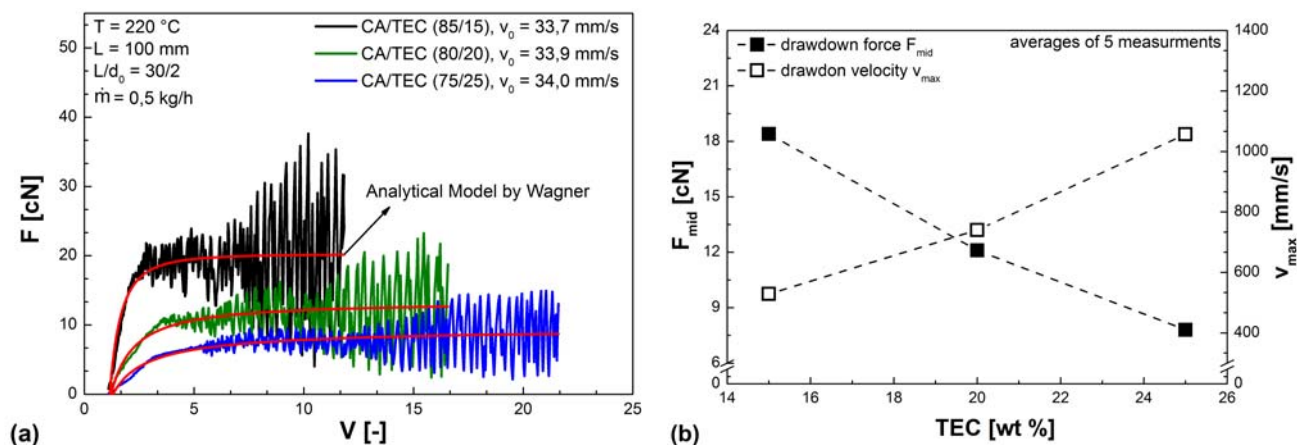
A master curve was produced using a concentration-dependent shift factor a_c similar to Gerhardt *et al.* [40]. The viscosity of CA plasticized with 15 wt % TEC was taken as the reference curve. The shift factor a_c was found to be 0.326 for 20 wt % TEC and 0.113 for 25 wt % TEC. The viscosity data of the master curve were additionally fitted using the Carreau-Yasuda model according to Equation (3) [41].

$$\eta = \eta_0 \cdot \left[1 + (\lambda \cdot \dot{\gamma})^a \right]^{\frac{n-1}{a}} \quad (3)$$

The Carreau-Yasuda model includes the zero shear viscosity η_0 , a time constant λ , the shear rate $\dot{\gamma}$, the power law exponent n , and a dimensionless parameter a , which describes the width of the transition between the zero shear viscosity region and the power law region.

However, many polymer processing technologies such as foam extrusion involves not only shear flows but also elongational flows. Uniaxial elongational flow properties of externally plasticized CA were investigated using the Rheotens test. Figure 7a shows the drawdown force as a function of draw ratio. The Rheotens curves were successfully fitted using an analytical model developed by Wagner *et al.* [31] and a Levenberg-Marquardt procedure. Figure 7b shows the mean melt strength (mean drawdown force F_{mid}) and the maximum drawdown velocity as a function of TEC content. As can be seen from Figure 7a,b, maximum drawdown velocity and draw ratio increase with increasing plasticizer content while the drawdown force (melt strength) steadily decreases. The higher the plasticizer content the higher the chain mobility and the stronger the dilution effect. As a consequence, cellulose acetate chains are easily disentangled and aligned in drawdown direction causing an improvement in melt flow behavior accompanied with an increase in melt elongation and decrease in melt strength. Sungsanit [42] studied the effect of poly(ethylene glycol) (PEG) on elongational flow properties of poly(lactic acid) (PLA). He also noticed a decrease in melt strength and an increase in melt elongation of PLA with increasing PEG content.

Figure 7. (a) Drawdown force F as a function of draw ratio V in dependence of TEC content; (b) Mean drawdown force F_{mid} and maximum drawdown velocity v_{max} as function of TEC content.



From the fitted parameters of the analytical model, the elongational viscosity can be calculated according to Wagner *et al.* [31]. Figure 8 shows the apparent elongational viscosity of externally plasticized CA as a function of the extension rate. In the first part of the curves, the elongational viscosity steadily increases with increasing extension rate to reach a maximum (strain hardening). After this maximum, the elongational viscosity continuously decreases with higher extension rates according to the analytical model (power-law function). An increasing amount of TEC continuously increases the extension rate and slightly shifts the maximum (strain hardening) to higher extension rates. The total level of the elongational viscosity curve also decreases with increasing TEC content.

Only limited strain hardening is observed due to the high amount of plasticizer in CA. The slope of the elongational thinning region (power-law region) seems to be independent from the plasticizer concentration. Sungsanit [42] observed similar results upon investigating the elongational viscosity from Rheotens test of externally plasticized PLA.

Figure 8. Apparent elongational viscosity of externally plasticized CA as a function of extensional rate calculated using the analytical model developed by Wagner *et al.* [31] in comparison to shear viscosity at low shear rate.

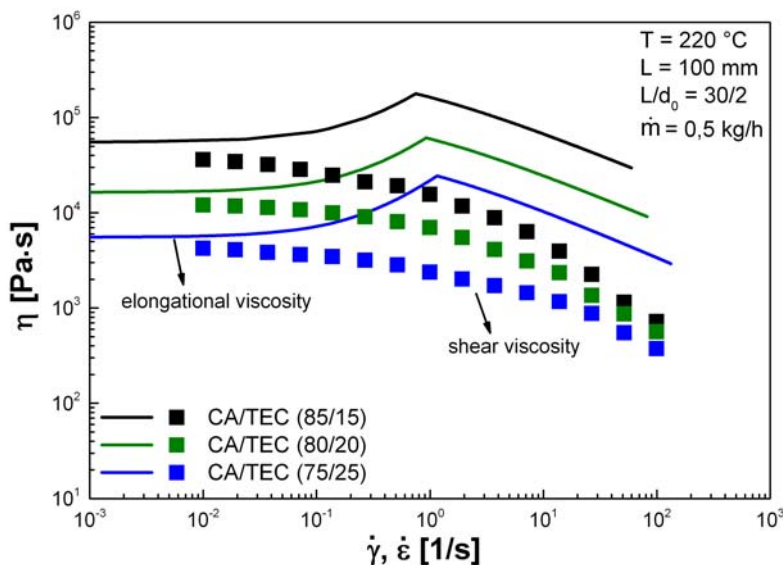
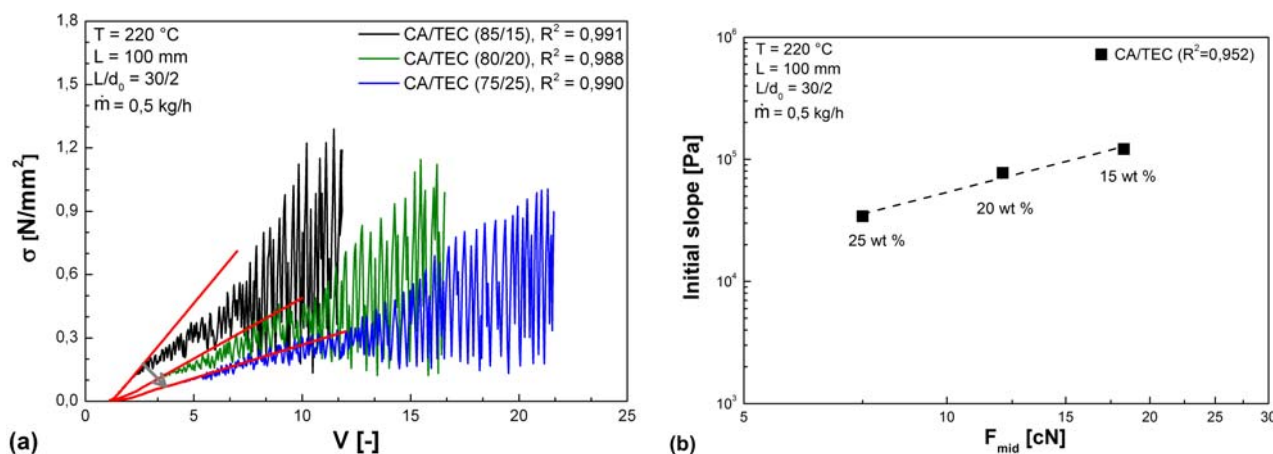


Figure 9. (a) Influence of TEC content on the stress curves σ as a function of draw ratio V ; (b) Initial slope of the stress curves σ via mean drawdown force F_{mid} .



In addition to elongational viscosity, the initial slope of the stress curve $\sigma(V)$ at low draw ratio V was also investigated. In the region of the initial slope the melt strand is exposed to low deformation rates similar to the strain hardening region in extensional viscosity measurements [32]. As shown in Figure 9, the initial slope decreases with increasing TEC content. This is in good agreement with the decreasing elongational viscosity from Figure 8. There seems to be a close relationship between plasticizer content, mean drawdown force F_{mid} , and the initial slope of the Rheotens curve within this study. Consequently, lower melt strength results in a lower initial slope. To verify this trend more

plasticizer concentrations as well as additional plasticizer types would have to be tested. Muke *et al.* [32] found a similar correlation between melt strength and the initial slope for polypropylene (PP). However, they reported that the initial slope is highly sensitive to the polymer grade, the weight of the strand, and the selected test conditions such as acceleration rate or distance L .

Muke *et al.* [32] and Lau *et al.* [43] investigated the relationship between melt strength and zero shear viscosity for PP. They described the relationship by a linear regression. Similar correlation is found in our study for externally plasticized CA, as shown in Figure 10. Melt strength decreases with decreasing zero shear viscosity. At low plasticizer content viscosity is high, thus cellulose acetate chains tend to have higher resistance to extensional deformation. In other words, the higher the plasticizer content the stronger the dilution effect and the lower the viscosity of externally plasticized CA. Disentanglement of cellulose acetate chains under extensional flow is facilitated yielding lower zero shear viscosity and lower melt strength. However, further studies are required using additional plasticizer concentrations and further plasticizer types to verify this trend.

Figure 10. Maximum drawdown force F_{max} and mean drawdown force F_{mid} of externally plasticized CA via zero shear viscosity η_0 .

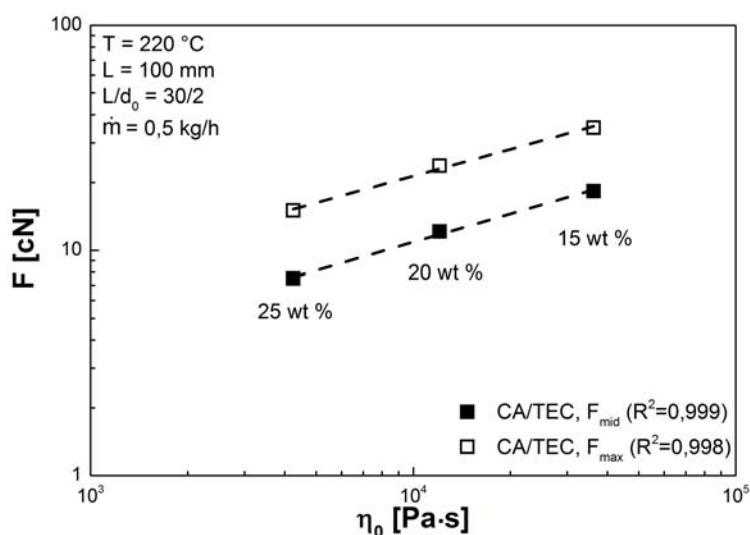


Table 4 summarizes important rheological characteristics of externally plasticized CA in dependence of TEC content. The Hencky strain ϵ_H was obtained from the draw ratio V using Equation (4).

$$\epsilon_H = \ln\left(\frac{v}{v_0}\right) \tag{4}$$

The strain hardening behavior SH was estimated according to Equation (5) [41]:

$$SH = \frac{\eta_e}{3\eta_0} \tag{5}$$

where η_e (Pa·s) is the apparent elongational viscosity obtained from the initial slope of the elongational viscosity curves (Figure 8) similar to Sungsanit [42] and η_0 (Pa·s) is the zero shear viscosity measured by means of rotational rheometer. It can be seen from Table 4 that zero shear viscosity, melt strength,

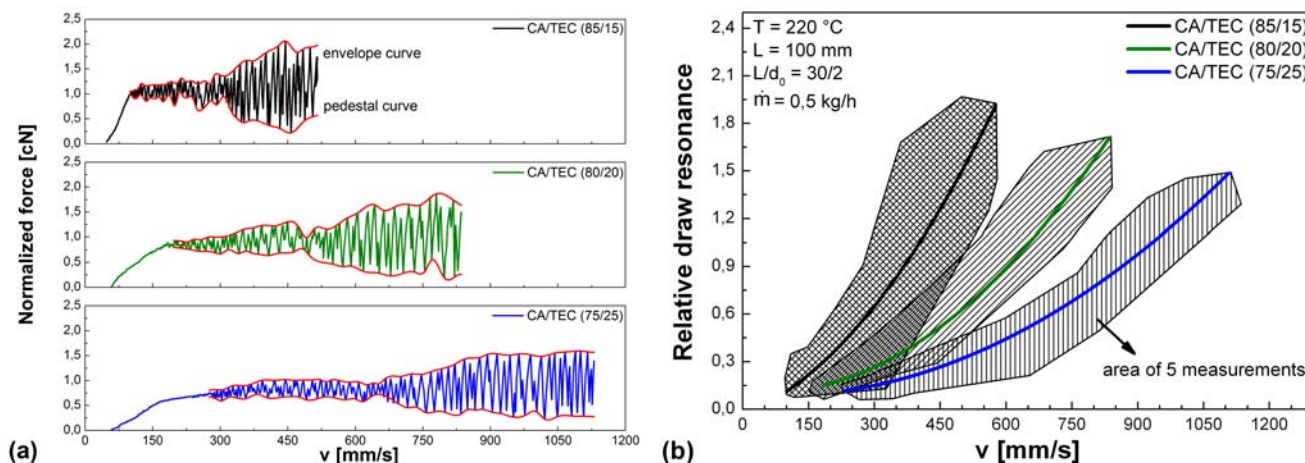
and strain hardening decrease whereas melt flow rate, drawability and Hencky strain increase with increasing plasticizer content.

Table 4. Melt flow rate, zero shear viscosity, Rheotens characteristics, Hencky strain, and strain hardening behavior of externally plasticized CA (average values of five measurements).

Property	TEC (wt %)		
	15	20	25
MFR (g/10 min)	2.2	5.7	11.8
η_0 (Pa·s)	36210	12060	4250
F_{max} (cN)	35.0	23.7	15.0
F_{mid} (cN)	18.3	12.1	7.5
F_{min} (cN)	4.3	3.4	2.3
v_{max} (mm·s ⁻¹)	528.5	758.1	1056.6
V_{max} (-)	12.1	16.2	21.6
ε_H (-)	2.5	2.8	3.1
SH (-)	1.7	1.4	1.2

The typical draw resonance of the Rheotens curves at higher drawdown velocities was studied by Steffl [44] for different polyethylene types under different test conditions. Consequently, we also investigated in our study the draw resonance with respect to plasticizer concentration. In a first step, the normalized drawdown force was calculated from the mean drawdown force F_{mid} . Then the draw resonances of these normalized Rheotens flow curves were covered by an envelope curve (maxima) and a pedestal curve (minima) similar to Steffl [44]. This is exemplarily shown in Figure 11a. The difference between the envelope curve and the pedestal curve is then defined as the relative draw resonance, as shown in Figure 11b. This procedure was done for all five measurements at each TEC concentration. From Figure 11 it can be seen that the draw resonance shifts to higher drawdown velocities v and its amplitude decreases with increasing TEC content. This can be explained by the higher chain mobility and stronger dilution effect with increasing amount of TEC in CA.

Figure 11. (a) Normalized drawdown force F as a function of drawdown velocity v in dependence of TEC content; (b) Relative draw resonance as a function of drawdown velocity v in dependence of TEC content (scattered area covers five measurements).



When discussing the usability of externally plasticized CA for foam extrusion, investigation of the area under the Rheotens curve is important. This was found by Stadlbauer *et al.* [36] who defined a foamability number FN from the integral of the drawdown force as a function of draw ratio. They correlated this foamability number to the foaming performance and found that a higher foamability number leads to lower foam densities and improved foaming. However, Stadlbauer *et al.* [36] did not consider the throughput in their calculation. Consequently, in our study we included the throughput of the extruder to obtain a specific energy input ΔG per unit mass of the material. The specific energy input per unit mass was calculated at maximum drawdown velocity v_{\max} (with $v_0 = 0$) from the mean drawdown force F_{mid} multiplied with the maximum drawdown velocity v_{\max} (Integral) and divided by the throughput \dot{m} of the extruder according to Equation (6).

$$\Delta G = \frac{F_{\text{mid}} \cdot (v_{\max} - v_0)}{\dot{m}} \text{ (J} \cdot \text{g}^{-1}\text{)}, \text{ with } v_0 = 0 \quad (6)$$

The specific energy input in viscoelastic melts describes the ability of the melt to partly absorb and store deformation energy as well as to partly transform it, for example into heat. For a high energy input per unit mass, the area under Rheotens curve must be maximized (optimized ratio between drawdown force and drawdown velocity). Table 5 shows the estimated specific energy input at maximum drawdown velocity as well as the foamability number at maximum draw ratio calculated according to Stadlbauer *et al.* [36].

Table 5. Specific energy input per unit mass at maximum drawdown velocity and foamability number at maximum draw ratio of externally plasticized CA.

Property	TEC (wt %)		
	15	20	25
ΔG at v_{\max} ($v_0 = 0$) ($\text{J} \cdot \text{g}^{-1}$)	0.70	0.66	0.57
FN at V_{\max} (N)	2.21	1.96	1.62

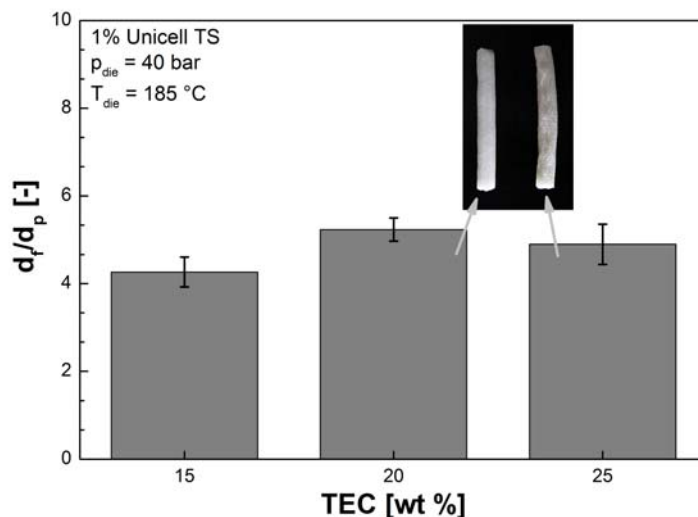
As shown in Table 5, the plasticizer content influences the foamability number and the rate of energy input per unit mass. When the plasticizer content is increased to 25 wt %, the specific energy input and the foamability number decrease continuously. This decrease seems to be more pronounced when the plasticizer content is increased from 20 to 25 wt %. It becomes clear that with increasing plasticizer concentration the dilution effect exceeds the plasticization effect, *i.e.*, above 20 wt % the surplus plasticizer, which is not in direct interaction to the polar groups of the molecules, acts as a lubricant. Preliminary foam extrusion tests using chemical blowing agents were conducted to verify the results from rheological characterization.

3.3. Influence of Plasticizer Content on Foam Extrusion Behavior of CA

The foam extrusion tests are in good agreement with the results from the rheological characterization. Figure 12 shows the expansion ratio as a function of plasticizer content. At low and high plasticizer content slightly lower expansion ratios of the final strands are observed. On one hand when plasticizer content is too low, melt strength and viscosity increase too fast at the die preventing full expansion of the strand. On the other hand, when the plasticizer content in CA is too high, melt

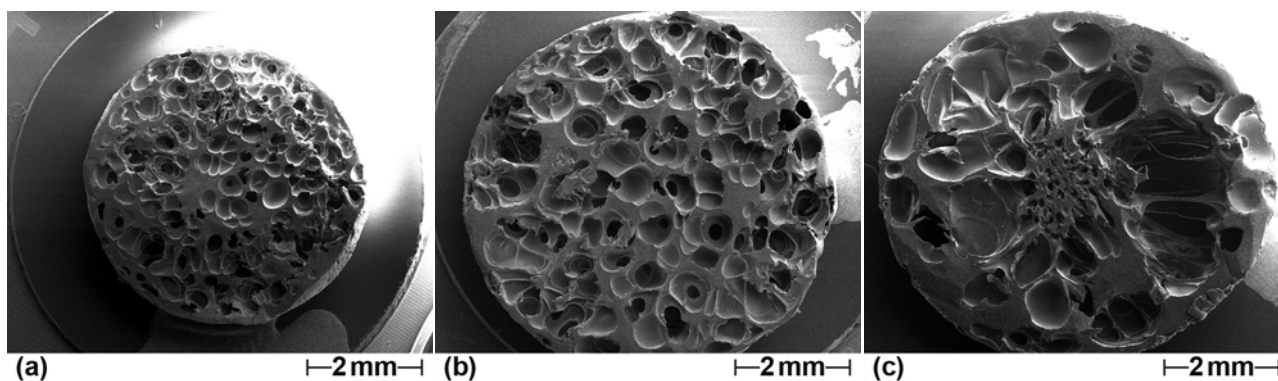
strength and viscosity are too low at the extrusion temperature used in this study. Consequently, cell wall rupture followed by foam collapse and shrinkage of the strand are observed.

Figure 12. Expansion ratio d_f/d_p of extrusion foamed CA strands using 1% Unicell TS at 40 bar as a function of TEC content.



SEM images in Figure 13 confirm the results from the rheological characterization and the expansion behavior at die, too. At 25 wt % TEC inhomogeneous foam morphology with large partially open cells is observed. Finer foam morphology with more homogenous cell size distribution is found with decreasing plasticizer content due to increasing melt strength and viscosity. No significant difference in foam morphology is found for 15 wt % TEC and 20 wt % TEC. However, as seen in Figure 12, too low plasticizer content leads to incomplete expansion due to strong viscosity and melt strength increase at the die. From the rheological properties and the foaming performance of externally plasticized CA, an optimum TEC content seems to be between 15 and 20 wt % within this study.

Figure 13. Influence of plasticizer content on foam morphology of CA (1% Unicell TS, p_{die} 40 bar, T_{die} 185 °C): (a) 15 wt % TEC; (b) 20 wt % TEC; and (c) 25 wt % TEC.



4. Conclusions

Shear viscosity and elongational flow properties of externally plasticized CA in dependence of plasticizer content were investigated. The plasticizer, triethyl citrate (TEC), was used in three

concentrations. Shear viscosity decreases with increasing plasticizer content. A master curve was produced using a concentration-dependent shift factor. This master curve was fitted using the Carreau-Yasuda model. Uniaxial elongational flow properties were studied using the Rheotens test. The analytical model proposed by Wagner was successfully applied to calculate the elongational viscosity from the Rheotens curves. An increase in TEC content leads to a steady decrease in melt strength (drawdown force) and elongational viscosity while melt extensibility (drawability) continuously increased. The observed elongational flow properties of externally plasticized CA are excellent with respect to foam extrusion. Melt strength and melt extensibility are comparable with values for standard foam polymers even at high TEC contents of 20 to 25 wt %. Since zero shear viscosity is directly influenced by the plasticizer content, close relationship between zero shear viscosity and melt strength is observed. The typical draw resonance shifts to higher drawdown velocity and the amplitude of the draw resonance decreases with increasing TEC content. Foamability number at maximum draw ratio and specific energy input per unit mass at maximum drawdown velocity were calculated from the area under the Rheotens curves in dependence of TEC content. Both decrease with increasing plasticizer content. This effect was more pronounced from 20 to 25 wt % TEC indicating stronger dilution.

Preliminary foam extrusion tests using chemical blowing agents were conducted to verify the rheological characterization. When plasticizer content is too high, foam collapse and inhomogeneous morphology with large partially open cells are observed. Good foam extrusion behavior and more homogenous foam morphologies are achieved at lower plasticizer content. However, when TEC content is too low, melt strength and viscosity seem to increase too quickly prohibiting full expansion of the strand after the die. The tests show that high melt strength is necessary but not the only criterion for good foaming. In addition, elongational viscosity as well as the ratio between melt strength and melt extensibility (area under the Rheotens curve) have to be taken into account. With respect to these results, an optimal TEC content can be assumed around 20 wt %, where a good balance between rheology and foaming behavior of cellulose acetate is achieved. It is well-known that the performance of a plasticizer is closely linked to its compatibility and miscibility with the polymer. Therefore, further plasticizers will be studied and compared to the results obtained in this study. Additionally, foam extrusion tests with physical blowing agents will be conducted to investigate the foaming behavior of externally plasticized CA in detail.

Acknowledgments

This work was funded by the Federal Ministry of Food, Agriculture and Consumer Protection BMELV and the Agency for Renewable Resources FNR (FKZ: 22023106). The authors thank Jungbunzlauer AG for plasticizer supply, Acetati SpA for providing the cellulose acetate, and Tramaco GmbH for chemical blowing agent supply. Special thanks go to M. H. Wagner for his valuable discussion of the Rheotens test and its interpretation.

References

1. Zhang, Q.; Xanthos, M. Material Properties Affecting Extrusion Foaming. In *Polymeric Foams: Mechanisms and Materials*; Lee, S.-T., Ramesh, N.S., Eds.; CRC Press: Boca Raton, FL, USA, 2004; Chapter 4, pp. 111–138.
2. Gendron, R. Rheological Behavior Relevant to Extrusion Foaming. In *Thermoplastic Foam Processing: Principles and Development*; Gendron, R., Ed.; CRC Press: Boca Raton, FL, USA, 2005; Chapter 2, pp. 43–103.
3. Kwag, C.; Manke, C.W.; Gulari, E. Effects of dissolved gas on viscoelastic scaling and glass transition temperature of polystyrene melts. *Ind. Eng. Chem. Res.* **2001**, *40*, 3048–3052.
4. Lee, M.; Park, C.B.; Tzoganakis, C. Measurements and modeling of PS/supercritical CO₂ solution viscosities. *Polym. Eng. Sci.* **1999**, *39*, 99–109.
5. Gendron, R.; Daigneault, L.E.; Caron, L.M. Rheological behavior of mixtures of polystyrene with HCFC 142b and HFC 134a. *J. Cell. Plast.* **1999**, *35*, 221–246.
6. Tatibouët, J. Investigating Foam Processing. In *Thermoplastic Foam Processing: Principles and Development*; Gendron, R., Ed.; CRC Press: Boca Raton, FL, USA, 2005; Chapter 5, pp. 192–234.
7. Lee, S.-T. Foam Nucleation in Gas-Dispersed Polymeric Systems. In *Foam Extrusion: Principles and Practice*; Lee, S.-T., Ed.; CRC Press: Boca Raton, FL, USA, 2000; Chapter 4, pp. 81–124.
8. Stange, J. Einfluss rheologischer Eigenschaften auf das Schäumverhalten von Polypropylenen unterschiedlicher molekularer Struktur. Ph.D. Dissertation, Friedrich-Alexander University, Erlangen-Nürnberg, Germany, 2006.
9. Gunkel, F.; Spörrer, A.N.J.; Lim, G.T.; Bangarusampath, D.S.; Altstädt, V. Understanding melt rheology and foamability of polypropylene-based TPO blends. *J. Cell. Plast.* **2008**, *44*, 307–325.
10. Xanthos, M.; Yilmazer, U.; Dey, S.K.; Quintans, J. Melt viscoelasticity of polyethylene terephthalate resins for low density extrusion foaming. *Polym. Eng. Sci.* **2000**, *40*, 554–566.
11. Bergamaschi, E.; Smargiassi, A.; Mutti, A.; Franchini, I.; Lucchini, R. Immunological changes among workers occupationally exposed to styrene. *Int. Arch. Occup. Environ. Health* **1995**, *67*, 165–171.
12. Guillemin, M.P.; Berode, M. Biological monitoring of styrene: A review. *Am. Ind. Hyg. Assoc. J.* **1988**, *49*, 497–505.
13. Anttila, A.; Bhat, R.V.; Bond, J.A.; Borghoff, S.J.; Bosch, F.X.; Carlson, G.P.; Castegnaro, M.; Cruzan, G.; Gelderblom, W.C.A.; Hass, U.; *et al.* Styrene. In *IARC Monographs on the Evaluation of Carcinogenic Risks to Humans: Some Traditional Herbal Medicines, Some Mycotoxins, Naphthalene and Styrene*; International Agency for Research on Cancer (IARC) Press: Lyon, France, 2002; Volume 82, pp. 437–550.
14. Cherry, N.; Gautrin, D. Neurotoxic effects of styrene: Further evidence. *Br. J. Ind. Med.* **1990**, *47*, 29–37.
15. Edgar, K.J.; Buchanan, C.M.; Debenham, J.S.; Rundquist, P.A.; Seiler, B.D.; Shelton, M.C.; Tindall, D. Advances in cellulose ester performance and applications. *Prog. Polym. Sci.* **2001**, *26*, 1605–1688.

16. Mohanty, A.K.; Wibowo, A.; Misra, M.; Drzal, L.T. Development of renewable resource-based cellulose acetate bioplastics: Effect of process engineering on the performance of cellulosic plastics. *Polym. Eng. Sci.* **2003**, *43*, 1151–1161.
17. Wypych, G. Plasticizers Use and Selection for Specific Polymers. In *Handbook of Plasticizers*; Wypych, G., Ed.; ChemTec Publishing: Toronto, Canada, 2004; Chapter 11, pp. 273–379.
18. Fridman, O.A.; Sorokina, A.V. Criteria of efficiency of cellulose acetate plasticization. *Polym. Sci. B* **2006**, *48*, 233–236.
19. Zepnik, S.; Kabasci, S.; Radusch, H.-J.; Wodke, T. Influence of external plasticization on rheological and thermal properties of cellulose acetate with respect to its foamability. *J. Mater. Sci. Eng. A* **2012**, *2*, 152–163.
20. Das, M. Effect of screw speed and plasticizer on the torque requirement in single screw extrusion of starch based plastics and their mechanical properties. *Indian J. Chem. Technol.* **2008**, *15*, 555–559.
21. Jiugao, Y.; Ning, W.; Xiaofei, M. The effects of citric acid on the properties of thermoplastic starch plasticized by glycerol. *Starch/Stärke* **2005**, *57*, 494–504.
22. Shah, B.L.; Shertukde, V.V. Effect of plasticizers on mechanical, electrical, permanence, and thermal properties of poly(vinyl chloride). *J. Appl. Polym. Sci.* **2003**, *90*, 3278–3284.
23. Gil, N.; Negulescu, I.; Saska, M. Evaluation of the effects of bio-based plasticizers on thermal and mechanical properties of poly(vinyl-chloride). *J. Appl. Polym. Sci.* **2006**, *102*, 1366–1373.
24. Marcilla, A.; Beltrán, M. Mechanisms of Plasticizers Action. In *Handbook of Plasticizers*; Wypych, G., Ed.; ChemTec Publishing: Toronto, Canada, 2004; Chapter 5, pp. 107–120.
25. Qian, J.W.; Rudin, A.; Teh, J.W. Effects of plasticizer on shear modification of polystyrene. *Polym. Int.* **1991**, *24*, 165–171.
26. Ghanbarzadeh, B.; Oromiehie, A.; Musavi, M.; Razmi, E.; Milani, J. Effect of polyolic plasticizers on rheological and thermal properties of zein resins. *Iran. Polym. J.* **2006**, *15*, 779–787.
27. Sungsanit, K.; Kao, N.; Bhattacharya, S.N.; Pivsaart, S. Physical and rheological properties of plasticized linear and branched PLA. *Korea-Aust. Rheol. J.* **2010**, *22*, 187–195.
28. Lin, C.-A.; Ku, T.-H. Shear and elongational flow properties of thermoplastic polyvinyl alcohol melts with different plasticizer contents and degrees of polymerization. *J. Mater. Process. Technol.* **2008**, *200*, 331–338.
29. Hansen, C.M. *Hansen Solubility Parameters: A User's Handbook*, 2nd ed.; CRC Press: Boca Raton, FL, USA, 2007.
30. Villmow, T.; Kretschmar, B.; Pötschke, P. Influence of screw configuration, residence time, and specific mechanical energy in twin-screw extrusion of polycaprolactone/multi-walled carbon nanotube composites. *Compos. Sci. Technol.* **2010**, *70*, 2045–2055.
31. Wagner, M.H.; Bernnat, A.; Schulze, V. The rheology of the rheotens test. *J. Rheol.* **1998**, *42*, 917–928.
32. Muke, S.; Ivanov, I.; Kao, N.; Bhattacharya, S.N. The melt extensibility of polypropylene. *Polym. Int.* **2001**, *50*, 515–523.
33. Kao, N.; Chandra, A.; Bhattacharya, S. Melt strength of calcium carbonate filled polypropylene melts. *Polym. Int.* **2002**, *51*, 1385–1389.

34. Spoerrer, N.J.; Bangarusampanth, D.S.; Altstädt, V. The Challenge of Foam Injection-Moulding Possibilities to Improve Surface Appearance, Foam Morphology and Mechanical Properties. In Proceedings of the 9th International Conference on Blowing Agents and Foaming Processes, Frankfurt, Germany, 22–23 May 2007; Paper 16.
35. Bernnat, A. Polymer Melt Rheology and the Rheotens Test. Ph.D. Dissertation, University of Stuttgart, Stuttgart, Germany, 2001.
36. Stadlbauer, M.; Folland, R.; DeMink, P. Extruded Polyolefin for the Manufacture of Cellular Material. Eur. Pat. 1816158 A1, 8 August 2007.
37. Mitrus, M. Changes of specific mechanical energy during extrusion cooking of thermoplastic starch. *TEKA Kom. Mot. Energ. Roln.* **2005**, *5*, 152–157.
38. Van der Burgt, M.C.; van der Woude, M.E.; Janssen, L.P.B.M. The influence of plasticizer on extruded thermoplastic starch. *J. Vinyl Addit. Technol.* **1996**, *2*, 170–174.
39. Guerrero, P.; Beatty, E.; Kerry, J.P.; de la Caba, K. Extrusion of soy protein with gelatin and sugars at low moisture content. *J. Food Eng.* **2012**, *110*, 53–59.
40. Gerhardt, L.J.; Manke, C.W.; Gulari, E. Rheology of polydimethylsiloxane swollen with supercritical carbon dioxide. *J. Polym. Sci. B Polym. Phys.* **1997**, *35*, 523–534.
41. Dealy, J.M.; Larson, R.G. *Structure and Rheology of Molten Polymers: From Structure to Flow Behavior and Back Again*; Hanser Publishers: Munich, Germany, 2006; pp. 329–413.
42. Sungsanit, K. Rheological and Mechanical Behaviour of Poly(lactic acid)/Polyethylene Glycol Blends. Ph.D. Dissertation, RMIT University, Melbourne, Australia, 2011.
43. Lau, H.C.; Bhattacharya, S.N.; Field, G.J. Melt strength of polypropylene: Its relevance to thermoforming. *Polym. Eng. Sci.* **1998**, *38*, 1915–1923.
44. Steffl, T. Rheological and Film Blowing Properties of Various Low Density Polyethylenes and Their Blends. Ph.D. Dissertation, Friedrich-Alexander University, Erlangen-Nürnberg, Germany, 2004.